Supersonic Flow of Nonuniform Freestreams past Aerodynamic Decelerators

FRANKIE G. MOORE*
Naval Weapons Laboratory, Dahlgren, Va.

AND

FRED R. DEJARNETTE†
North Carolina State University, Raleigh, N. C.

AND

EUGENE N. BROOKS JR.‡
Naval Ship Research and Development Center, Washington, D. C.

Flowfields past aerodynamic decelerators immersed in the wake of a primary vehicle are investigated analytically. Inviscid flowfields were computed by the methods of characteristics and integral relations, and laminar boundary-layer properties were calculated numerically. Results for pointed wedges and cones showed an adverse pressure gradient on the surface which led to boundary-layer separation in some cases and an inviscid surface Mach number going to unity for some wake profiles. Surface pressure distributions were found to correlate very well with the tangent cone approximation and reasonably well with a Newtonian theory applied to nonuniform freestreams.

Nomenclature

A = parameter used in specifying nonuniform freestream velocity defect in Eq. (1)
B = parameter used in specifying nonuniform freestream velocity distribution in Eq. (1)
C_D = drag coefficient, see Eq. (5)
C_f = skin-friction coefficient based on far freestream conditions see Eq. (3)
k = constant defined by Eq. (6)
L = cone length
M = Mach number
p = pressure
$\bar{p}$ = nondimensional pressure, $\bar{p} = p/\rho_\infty V_\infty^2$
q_w = heat-transfer rate at the wall, Btu/ft²-sec
Re = Reynolds number based on far freestream conditions
S = entropy
V = total velocity
x,y = coordinate along and normal to body axis of symmetry, see Fig. 1
y^* = shock-wave position on initial-data line
β = shock wave angle
γ = ratio of specific heats (1.4)
δ = body inclination angle with respect to body axis
θ = direction of velocity vector with respect to body axis of symmetry
ρ = density

Subscripts

b = body point
s = shock point
N = conditions at the nose ($y_1 = 0$)
∞ = far freestream condition at $y = \infty$
1 = local freestream condition at $y = y_1$

Presented as Paper 70-1176 at the AIAA Aerodynamic Deceleration Systems Conference, Dayton, Ohio, September 14–16, 1970; submitted September 21, 1970; revision received August 20, 1970. This research was partially supported by NASA Grant 47-004-006.

* Aerospace Engineer.
† Professor of Aerospace and Mechanical Engineering. Associate Fellow AIAA.
‡ Aerospace Engineer. Associate Member AIAA.

Introduction

ONE of the problems associated with the re-entry of a space vehicle into a planetary atmosphere is the design of a decelerator to slow the vehicle down to tolerable speeds. Aerodynamic decelerators, composed of light-weight high-drag bodies towed behind the primary vehicle, have been proposed to solve this problem. Since the decelerator follows in the wake of the primary vehicle, the freestream approaching the decelerator is nonuniform and similar to that shown in Fig. 1. The nonuniformity of this freestream has a substantial effect on both the drag and stability of a decelerator when compared to the corresponding results for a uniform freestream.

Various experimental and theoretical studies have been performed on towed right-circular cones[1–7] to assess their feasibility as a decelerator. These experimental results confirm that the static pressure in the far wake is nearly constant even though the velocity varies significantly.

This velocity variation causes other flowfield properties like Mach number (M_1), density (ρ_1), and entropy (S_1) to be nonuniform. In particular, a strong entropy layer exists which, in turn, passes over the decelerator as it moves through the wake. On the other hand, the total enthalpy may be considered to be approximately constant in the wake.[6]

Nerem[8] has shown that the tow cable changes the velocity profiles near the axis since there is a viscous layer associated with the cable itself. In addition, the tow cable may cause flow separation just upstream of the nose of the decelerator.[5] These effects are not considered in the present analysis which is concerned with the calculation of flowfields past pointed bodies immersed in wake-like nonuniform freestreams.

Sullivan et al,[9] used a linearized method of characteristics to solve the inviscid flowfield past small-angle wedges with a freestream Mach number profile similar to that approaching the flare on a cone-cylinder-flare configuration. However, this linearized solution is limited to very small wedge angles. George[10] obtained linearized perturbation solutions for plane and axisymmetric entropy layers over small angle wedges and flares.

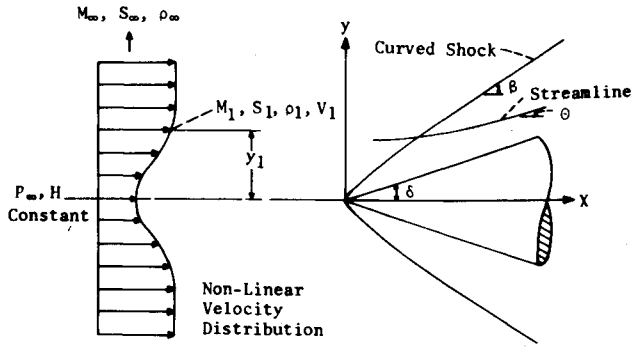

Fig. 1 Coordinate system and freestream properties.

In an unpublished M. S. thesis, the third author[11] used the first approximation (one strip) of Dorodnitsyn's Method of Integral Relations[12] to calculate the flowfield of the nonuniform freestream given by Eq. (1) past wedges and cones. Some of these results appear herein for comparison purposes. In an independent analysis, Barteneu and Shirshou[13] also used the one-strip method of integral relations to calculate nonuniform supersonic flows past pointed bodies of revolution. Since the flowfields produced by nonuniform freestreams are highly nonlinear, the results from the method of integral relations are questionable.

Inouye[14] used a combined inverse method-method of characteristics to calculate the inviscid flowfield past blunt axisymmetric bodies in a supersonic spherical source flow. Patterson and Lewis[14] used a somewhat similar approach to investigate nonuniform hypersonic freestreams about blunt axisymmetric bodies. However, the freestream velocity profiles for both of these analyses had the maximum velocity along the axis of symmetry, and the velocity decreased in the transverse direction. These velocity profiles are quite different from the wake-like profiles considered here.

The present paper applies the method of characteristics to calculate two-dimensional and axisymmetric flowfields past pointed bodies in nonuniform supersonic freestreams. Modifications are required, however, to the standard method of characteristics[16] to account for the nonuniform freestream properties at the shock wave and the entropy layer on the surface. Freestreams with wake-like profiles are used for a perfect gas ($\gamma = 1.4$) with the static pressure and total enthalpy constant in the freestream. Laminar boundary-layer properties are computed to check for boundary-layer separation and to determine skin-friction coefficients and heat-transfer rates. Approximate methods, based on tangent cone and Newtonian impact theories, are developed for the surface pressure coefficients. Results are presented for wedges in two-dimensional freestream profiles and cones in axisymmetric freestream profiles.

Analysis

Determination of Freestream Properties

Campbell[1] found that measured transverse velocity profiles for wakes behind cones in supersonic flow can be accurately represented by the relation

$$V_1/V_\infty = 1 - A \exp(-BY_1^2) \qquad (1)$$

where V_∞ is the wake velocity as $V_1 \to \pm \infty$, Y_1 is the distance perpendicular to the body axis (see Fig. 1), and A and B are parameters depending on the primary body shape and axial position relative to the wake. The first author[7] found that other mathematical models of the wake velocity profile yielded results similar to those using Eq. (1).

Equation (1) together with the assumptions of constant pressure and total enthalpy in the freestream are sufficient to determine all the other nondimensional properties in the nonuniform freestream.

Inviscid Flowfield Solution

There are several methods which could be used for the inviscid flowfield solution, depending on whether the shock wave is attached or not. If it is assumed that M_1 at $Y_1 = 0$ is large enough so that the shock wave is attached to the body, then the most accurate and well-known method for the solution is the method of characteristics. This is the method used here.

In order to apply the method of characteristics, the flowfield properties must be known along an initial data line. To determine this data, a small region of the freestream at the nose, of height y^*, is assumed to be uniform and have the same properties as those at $y_1 = 0$. This means that the small region near the nose is unaffected by the nonuniform part of the freestream, and hence the usual flowfield properties for a cone (or wedge) exist in this region. In this manner the flowfield properties are determined along an initial data line constructed from the shock at $y_1 = y^*$ along a line normal to the body.

The method of characteristics, as given by the slopes of the characteristic lines and compatibility conditions, Eq. 17.38 and 17.39 of Shapiro,[16] for nonisentropic flow is used here to calculate the flowfield properties. However, modifications are required at the shock wave and body, which are explained below.

Boundaries

The boundaries for the method of characteristics are the body surface and the shock wave. A mesh point on the surface is located by the simultaneous solution of the right-running characteristic line from a known mesh point off the surface and the equation of the body $y_b = f(x)$. Since the entropy on the surface and the flow inclination angle θ are known, the velocity can be found from the compatibility condition. This is the usual approach used in the method of characteristics; however, the strong entropy layer adjacent to the surface in the problems considered here caused large differences to exist for some properties between the surface and the next mesh point off the surface. When this occurs, linear and even quadratic interpolation of properties between these two points is not adequate, hence additional mesh points must be added to the characteristic mesh near the body surface. This problem is discussed more thoroughly in the Results and Discussion Section.

Calculation of shock points requires special attention, and since the method differs from the usual method of calculation, it is discussed in detail here. In essence, calculation of the shock point amounts to a double iteration for the nonuniform freestream as opposed to a single iteration in the uniform freestream case. The first iteration is performed as though the freestream were uniform. That is the shock wave is first extrapolated until it intersects the left-running characteristic drawn from point B in Fig. 2. However, in order to avoid the intersection from occurring too far downstream, a point C is generally found by linearly interpolating the properties between points A and B. Then the left-running characteristic is drawn from point C until it intersects the extrapolated shock wave at point D. Knowing the value y_1 at point D, the freestream properties can be calculated from the equations derived above. Next, the velocity V_3, flow-inclination angle θ_3, and entropy S_3 just behind the shock wave are calculated from the shock jump conditions. Using θ_3 and S_3 and the compatibility conditions, a new velocity just behind the shock, say V_s, is calculated and compared with V_3. If V_s does not agree with V_3 within the accuracy desired, the velocity behind the shock is given the value

$$V_3' = (V_3 + V_s)/2$$

and this velocity and the freestream velocity V_1 at point D are used to calculate a new shock-wave angle β'. Then the remaining flowfield properties are computed from the shock jump conditions corresponding to β' and the freestream conditions at point D on Fig. 2. This procedure is then repeated until the desired accuracy between V_3 and V_s is obtained. However, the new location of the shock point is point E on Fig. 2, and unless point E is very close to point D the freestream properties at E are different from those at point D.

For the second part of the iteration scheme, if point E is not sufficiently close to point D, new freestream properties are computed at D using $y_1 = y_3'$ in Fig. 2. The entire iteration scheme is then repeated until the desired accuracy between points D and E in the second part of the iteration is obtained. Although a double iteration scheme is required, the technique converges very rapidly, and usually two or three iterations give an accuracy within $10^{-3}\%$ on velocity and shock location.

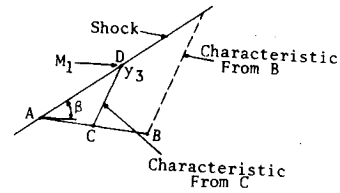

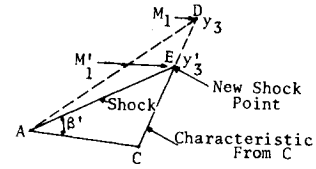

Fig. 2 Calculation of shock point.

Tangent Cone Approximation

As noted by Nerem[8] the tangent cone approximation, modified for the nonuniform freestream, should provide a reasonably accurate pressure distribution for pointed bodies in supersonic flows. If C_P^* is defined as the pressure coefficient based on local freestream conditions,

$$C_P^* = (p - p_\infty)/\tfrac{1}{2}\rho_1 V_1^2 \tag{2}$$

then C_P^* in the tangent cone approximation can be determined from Sim's cone tables[18] for the local value of δ and M_1. Then the pressure coefficient based on far freestream conditions is

$$C_P \equiv (p - p)/\tfrac{1}{2}\rho_\infty V_\infty^2 = C_P^* M_1^2/M_\infty^2 \tag{3}$$

This technique can be used to determine C_P at each body position.

Approximate Pressure Distribution from Newtonian Theory

At hypersonic speeds the Newtonian impact theory[17] has been found to yield reasonably accurate pressure distributions. Unlike the tangent cone approximation, it may be used for blunted as well as pointed bodies. The Newtonian pressure coefficient based on far freestream properties is

$$C_P = 2\sin^2\delta M_1^2/M_\infty^2$$

Love[19] has shown that a better approximation may be obtained by requiring the equation above to yield the correct value at the nose. The result here is

$$C_P = C_{P_N}^*(\sin^2\delta/\sin^2\delta_N)M_1^2/M_\infty^2 \tag{4}$$

where N refers to conditions at the nose ($y_1 = 0$). For blunt-nosed bodies $\sin\delta_N = 1$ and $C_{P_N}^*$ is the stagnation pressure coefficient based on freestream properties at $y_1 = 0$. In the case of pointed bodies with attached shock waves, $C_{P_N}^*$ is the wedge or cone C_P^* at the nose.

Equation (4) is used herein to compare with the method of characteristics and tangent cone pressure distributions over wedges and cones. However, it is more accurate for the blunt-nosed bodies than the pointed ones.

The Newtonian pressure drag-coefficient for the special case of a cone in the freestream velocity profile given by Eq. (1) is determined by integrating the pressure coefficient [Eq. (4)] as shown below

$$C_D = \frac{2}{L^2}\int_0^L C_P x dx = C_{P_N}^*\left\{1 + \frac{1}{2BL^2\tan^2\delta} \times \left[k(k+1)\ln\left(\frac{Ae^{-BL^2\tan^2\delta} - 1 + k}{A - 1 + k}\right) + k(k-1)\ln \times \left(\frac{Ae^{-BL^2\tan^2\delta} - 1 - k}{A - 1 - k}\right)\right]\right\} \tag{5}$$

where

$$k = \left[1 + \frac{2}{(\gamma - 1)M_\infty^2}\right]^{1/2} \tag{6}$$

L is the cone length, and $C_P = 0$ is used for the base of the cone.

Laminar Boundary-Layer Computations

As will be shown in the next section, wake-like velocity profiles produce adverse pressure gradients on the surfaces of wedges and cones. Therefore, solutions to the first-order laminar boundary-layer equations were obtained, using the finite-difference method described by Blottner[20] to check for possible boundary-layer separation and to determine skin friction coefficients and heat-transfer rates. The fact that the pressure gradient normal to the surface of a wedge or cone is zero gives some justification for using the first-order boundary-layer equations. All of the results were obtained for a perfect gas ($\gamma = 1.4$) with a Prandtl number of 0.70 and using Sutherland's viscosity formula. The wall temperature has a significant effect on the separation point, but the Reynolds number does not affect separation.

Results and Discussion

In order to start the method of characteristics the height of the uniform flow region y^* (discussed previously) and the flowfield properties along the initial data-line must be known. For a given value of y^*, the flowfield properties may be computed from the shock jump conditions (for a wedge) or the cone solution.[18]

A numerical study was performed to determine the effect of y^* on the solutions. For the freestream velocity profile given by Eq. (1), it was found that when $B = 10$ the solutions with $y^* = 0.01$ and $y^* = 0.001$ differed very little. However, significant differences were noted for the computational times since y^* establishes the height of the initial data line. Therefore, all the solutions presented here used $B = 10$ and $y^* = 0.01$.

The number of points on the initial data line must be chosen large enough to insure that the size of the characteristic mesh remains sufficiently small downstream, yet small enough to keep the computational time from being excessive. The number of points on the initial data line varied from 4–11 for the cases considered. As any of the parameters M_∞, A, or δ are increased the entropy difference between the body and the next mesh point off the surface increases, and the method of characteristics will not converge unless a finer mesh scale is used. The method of characteristics mentioned previously has V and S as dependent variables and uses linear interpolation between mesh points. Since the entropy variation is large in the problems considered here, several cases were also

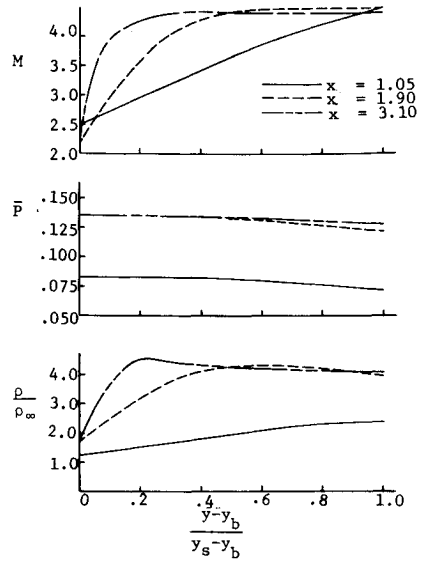

Fig. 3 Profiles of flow-properties normal to cone $M_\infty = 8.5$, $\delta = 20$, $A = 0.091$.

computed using the method of characteristics developed by Rakich,[21] which has p and θ as dependent variables and uses quadratic interpolation near the body. However, the results were very close to those obtained here, and that method also would not converge near the body unless more mesh points are added.

To illustrate the highly nonlinear nature of some flowfield properties Fig. 3 shows the Mach number, pressure, and density profiles normal to a cone for $M_\infty = 8.5$, $A = 0.091$, and $\delta = 20°$ at three streamwise positions. It is seen that the Mach number and density profiles are reasonably linear near the nose, but downstream these profiles become highly nonlinear. This nonlinearity is encompassed in an entropy layer near the surface which becomes progressively thinner downstream until finally as $x \to \infty$ an entropy singularity exists on the surface. On the other hand, Fig. 3 shows that the pressure profile has little variation, and in fact the pressure gradient normal to the surface is zero.

Another problem which arises, particularly for the larger values of δ and A, is that near the body the characteristic mesh size tends to increase in a direction normal to the body, whereas near the shock wave it increases in a direction parallel to the body. The local Mach number explains why, because the Mach number on the body is generally decreasing as x increases which means the Mach number just behind the shock wave increases as x increases which causes the slope of the Mach line there to decrease. These two problems can be solved by again adding more mesh points to the flowfield.

Several flowfields were computed for wedges and cones to determine the effect of M_∞ and the parameter A on the solution. The parameter B has no effect on the freestream nonuniformity other than to change the scale in the y_1-direction, so a value of 10 was used for all the cases herein. This value is completely arbitrary, however, since B always occurs in the product By_1^2, and a change in B is compensated by a change in y_1.

Figure 4a shows the nondimensional surface pressure, surface Mach number, and shock wave shape for a cone with $\delta = 20°$, $A = 0.1$ and several values of M_∞. Figure 5a gives the nondimensional pressure and surface Mach number for $M_\infty = 4$, $\delta = 20°$, and several values of A. The shock-wave angle β initially decreases as x increases until it reaches a minimum value and then increases and asymptotically approaches the value one would calculate for a completely uniform freestream at that value of M_∞. Although the shock-wave shapes are not shown for the cases given in Fig. 5a they follow the same general trends as those in Fig. 4a. The nondimensional pressure increases along the surfaces and approaches an asymptotic value corresponding to that for a completely uniform freestream. It is noticed that as M_∞ or A increases the adverse pressure gradients increase which may cause the boundary layer to separate; this point is discussed later. Since the surface pressure increases and the surface entropy for the inviscid solution is constant, the Mach number decreases along the surface until it too approaches an asymptotic value. However, this asymptotic value does not correspond to the Mach number for a completely uniform freestream because the surface entropy is determined from the shock-wave angle and freestream properties at the nose where $y_1 = 0$. On the other hand, the correct asymptotic value of the surface Mach number can be calculated from the asymptotic pressure and the surface entropy; these Mach number asymptotes are indicated on the figures.

Figure 5b presents the Mach number and nondimensional pressure along the surface of a wedge for $M_\infty = 4$, $A = 0.1$, and various wedge angles. It is interesting to note that the surface Mach number decreases as δ increases, and finally for $\delta = 30°$ the Mach number goes to unity at $x = 0.75$. Since the method of characteristics cannot compute subsonic flowfields, the solution was terminated at this point.

As an attempt to examine the flowfield more closely in cases where the inviscid flowfield appeared to have embedded subsonic regions, the one-strip method of integral relations was used since it is applicable to both subsonic and supersonic regions. However, it was found that for the cases in which the method of characteristics indicated a surface Mach number of one the profiles of flowfield properties normal to the surface were so nonlinear that the one-strip method of integral relations would not give adequate results. On the other hand the method of integral relations gives good results for freestreams with weak nonuniformities as shown in Fig. 4b. The Mach number predicted on the surface by the method of integral relations should be disregarded since the surface entropy is not held constant in that approach.

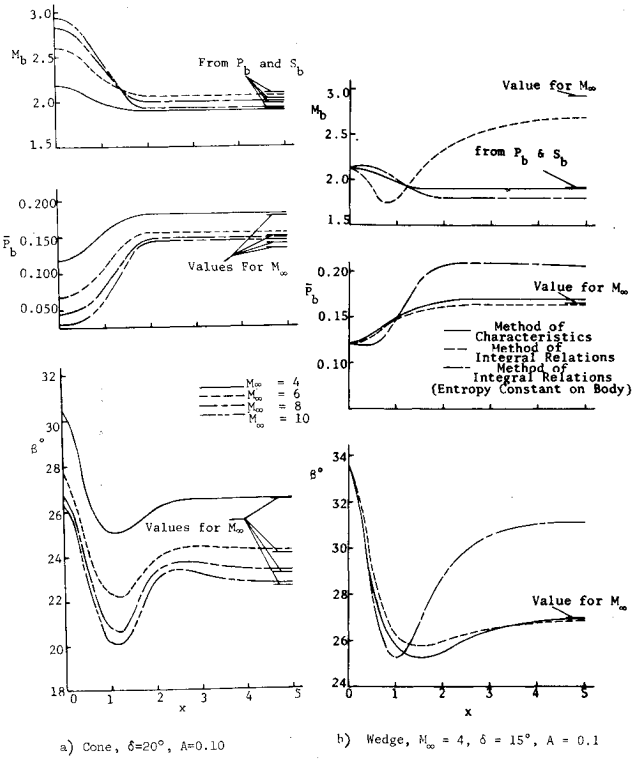

Fig. 4 Surface Mach number and pressure distribution and shock wave shape.

The third author[11] found that by holding entropy constant on the body (while disregarding the streamwise momentum equation), the one-strip method of integral relations yielded entirely different results than when the streamwise momentum equation was used and the entropy on the body allowed to vary. Comparing these results with the present method in Fig. 4b it is seen that much better agreement in shock shape and surface pressure is obtained if the entropy is allowed to vary on the body; however, the surface Mach number compares more favorably with the present method if the entropy on the body is constrained to be constant.

For all the cases computed, the computational time required by the method of characteristics was highly dependent on the number of points on the initial data line. Typical cases with four points on the initial data line required less than 3 min on an IBM 7040 computer, whereas cases with eleven points on the initial data line required up to 30 min. However this computer is relatively slow and much faster computational times could be obtained with the newer models of computers.

To show what a large effect these nonuniform freestreams have on the drag, and hence on the deceleration capabilities of a towed decelerator, the pressure distribution was numerically integrated over cones of various lengths (see Fig. 6).

The asymptotic values that the drag coefficients approach for large L are those that would be obtained for a cone in a uniform flow with the freestream conditions being those of the far freestream. It is seen that a detrimental reduction in drag by as much as 65% is encountered as a result of the nonuniform freestream and hence must certainly be accounted for in any design of a towed decelerator.

Also shown in Fig. 6, for comparison with the method of characteristics, are the tangent cone and Newtonian approximations to the pressure distribution and drag. It is seen that the tangent cone approximation gives very accurate results. This is quite significant because one can compute the remaining surface properties from the pressure and entropy and hence obtain an accurate solution for these properties with a minimum of computations. Moreover, computational time on the computer is approximately 2% of that for a corresponding case using the method of characteristics. A method such as this could be used very effectively in a boundary-layer program where the inviscid pressure along the body is required to compute the flowfield properties in the boundary layer.

On the other hand, the Newtonian approximations are not as accurate as the tangent cone method far back on the body. However, better results could be obtained by requiring the Newtonian pressure coefficient approach the asymptotic value far back on the body rather than that at the nose.

Figure 7 shows the surface Mach number and shock wave shape for the above case. Note that the Mach number goes to unity at $x = 0.86$ for the 30° cone. Hence the method of characteristics cannot continue beyond this point, but the tangent cone and Newtonian methods can still be applied.

As mentioned previously, the adverse pressure gradient on the surface of wedges and cones may cause boundary-layer separation. The laminar boundary-layer equations were solved numerically for several cases, using the method described previously, to investigate this possibility. For these computations, the units on x and y would be feet if the units on B were considered ($ft^{-1/2}$), because (By^2) is dimensionless. Consider the cases presented in Fig. 5b for wedges with $M_\infty = 4$, $A = 0.1$, and an adiabatic wall. The boundary layer for the 30° wedge was found to separate at $x \approx 0.70$, which is upstream of the point where the surface inviscid Mach number went to unity ($x \approx 0.75$). On the other hand, the wedges for $\delta = 15°$ and 20° did not experience boundary-layer separation. It is important to note that for all the wedge solutions in which the inviscid surface

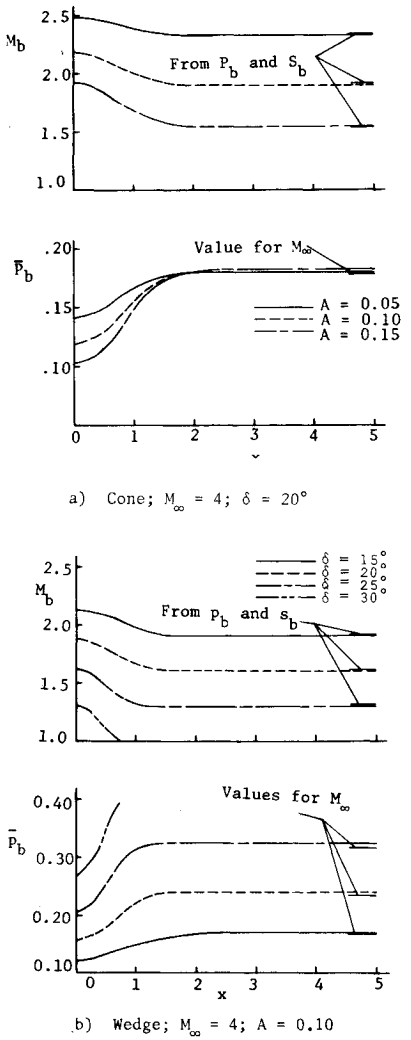

Fig. 5 Surface Mach number and pressure distributions for wedges. $M_\infty = 4$; $\delta = 15°, 20°, 25°, 30°$; $A = 0.10$.

Mach number went to unity, the boundary-layer separated upstream of the sonic point for the adiabatic wall condition. This means that the inviscid flowfield computations should be disregarded downstream of this point where separation occurs although the inviscid surface Mach numbers have not reached unity.

Figure 8 shows the skin friction coefficient for the same three cone angles ($\delta = 25°, 27.5°, 30°$) presented in Fig. 6

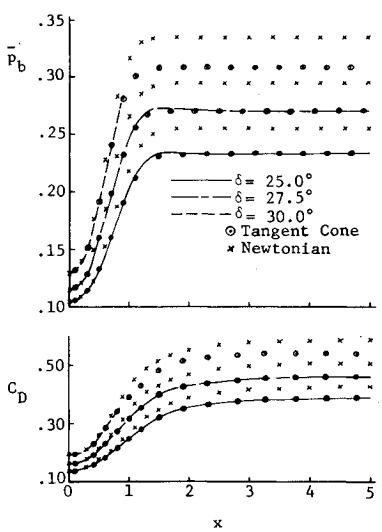

Fig. 6 Surface pressure and drag coefficient for cones. $M_\infty = 4.47$, $A = 0.1667$.

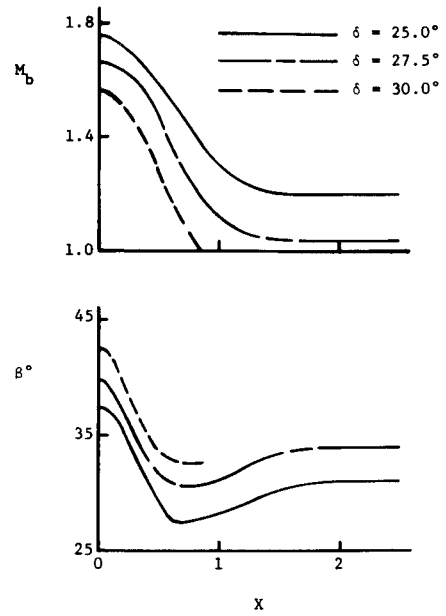

Fig. 7 Surface Mach number and shock wave shape for cones. $M_\infty = 4.47$; $A = 0.1667$.

and for an adiabatic wall. Note that the boundary layer not only separates on the 30° cone ($M_b = 1$ at $x = 0.86$) but on the 27.5° cone as well, even though an inviscid Mach number of unity was not reached on the surface. This verifies that one can indeed have boundary-layer separation in these nonuniform flowfields without the inviscid surface Mach number going to one.

In an effort to determine what effect a nonadiabatic wall would have on boundary-layer separation, solutions were obtained for the 30° cone with $T_w/T_o = 1.00$, 0.75, 0.50, and 0.25 where T_w is the wall temperature and T_o the freestream stagnation temperature. In this particular case the adiabatic wall corresponded to a value of $0.75 < T_w/T_o < 1.0$ so that the above four values for T_w/T_o represents successively colder values of the wall temperature. Figure 9 presents the heat transfer at the wall, q_w, where positive heat transfer is taken to be into the wall, and the local skin friction coefficient, C_f. It is seen that for the hot wall ($T_w/T_o = 1.0$) and relatively cool wall ($T_w/T_o = 0.75$) the boundary-layer separates, whereas for the cold wall ($T_w/T_o = 0.5$) and very cold wall ($T_w/T_o = 0.25$) the boundary layer remains attached. As might be expected the relatively hot wall dissipates heat into the freestream (q_w negative) whereas in the other three cases ($T_w/T_o = 0.75$, 0.5, and 0.25), the wall is being heated. Thus, here, as in the case of a wedge, the boundary layer is seen to separate upstream of the point where the inviscid surface Mach number went to unity for an adiabatic wall and also for a relatively cool wall. Although the Re/ft in Figs. 8 and 9 is excessive for laminar

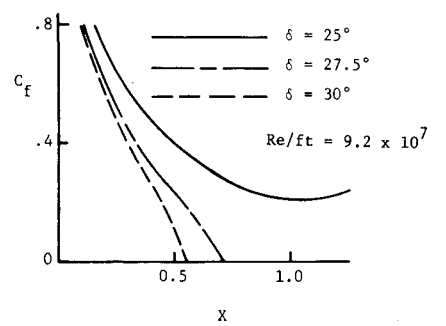

Fig. 8 Skin-friction coefficient for cones with adiabatic wall. $M_\infty = 4.47$; $A = 0.1667$.

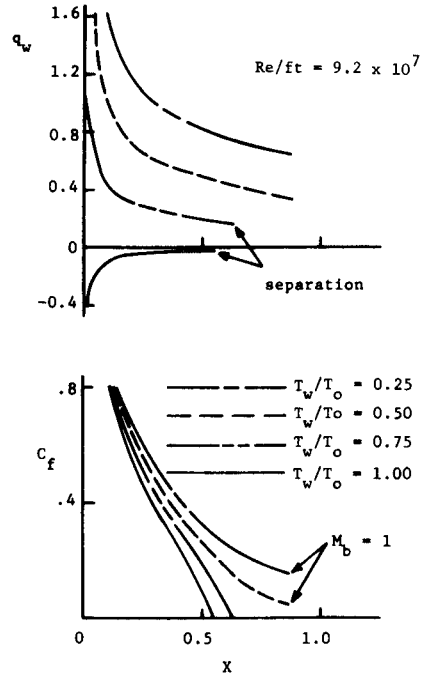

Fig. 9 Heat-transfer and skin-friction coefficient for a cone. $M_\infty = 4.47$; $A = 0.1667$, $\delta = 30°$.

boundary layers, the Reynolds number does not affect the calculated laminar separation point and these results are qualitatively correct for smaller Reynolds numbers.

Conclusions

1) The method of characteristics can be used to solve the inviscid flowfield past pointed bodies with attached shock waves in nonuniform freestreams representative of wakes. Modifications are required, however, at the shock wave to account for the nonuniform freestream and also near the body due to a strong entropy layer.

2) Typical results for wedges and cones show that the shock-wave angle decreases near the nose until it reaches a minimum value, then it increases and asymptotically approaches the angle corresponding to a completely uniform freestream. An adverse pressure gradient occurs along the surface in the nose region, after which the pressure asymptotically approaches the value for a uniform freestream. The surface Mach number decreases and asymptotically approaches a value much lower than that of the completely uniform freestream.

3) For some of the inviscid wedge and cone solutions the surface Mach number went to unity.

4) Because of the adverse pressure gradient, the laminar boundary layer separated on several of the wedge and cone cases. In addition, all cases where the inviscid Mach number went to unity were found to experience boundary-layer separation upstream of that point if the wall was assumed to be either adiabatic or relatively cool ($T_w/T_o = 0.75$).

5) Compared with the method of characteristics, the one-strip method of integral relations yields accurate results for the shock shape and surface pressure for freestreams with a weak nonuniformity. However, the surface Mach number is not accurate using that approach; and when highly nonuniform freestreams are used, all the flowfield properties are inaccurate.

6) The tangent cone approximation gave excellent results for properties on the body and at a reduction in computational time of about 98% over the method of characteristics.

7) An approximate equation for the pressure coefficients derived from Newtonian theory for nonuniform freestreams was found to yield reasonably accurate results for wedges

and cones. However, more accurate results could be obtained for blunt-nosed bodies.

8) For cones used as decelerators, large drag reductions can be realized due to the wake-like nonuniform freestreams.

References

[1] Campbell, J. F. and Graw, J. W., "Experimental Flow Properties in the Wakes of a 120° Cone at Mach Number 2.20," TN D-5365, July 1969, NASA.

[2] Charczenko, N. and McShera, J. T., "Aerodynamic Characteristics of Towed Cones Used as Decelerators at Mach Numbers from 1.57 to 4.65," TN D-994, 1961, NASA.

[3] Coats, J. D., "Static and Dynamic Testing of Conical Decelerators for the Pershing Re-Entry Vehicle," AEDC-TN-60-188, U.S. Air Force, Oct. 1960, Arnold Engineering Development Center, Tullahoma, Tenn.

[4] McShera, J. T., "Aerodynamic Drag and Stability Characteristics of Towed Inflatable Decelerators at Supersonic Speeds," TN D-1601, 1963, NASA.

[5] Reding, J. P. and Ericsson, L. E., "Loads on Bodies in Wakes," *Journal of Spacecraft and Rockets*, Vol. 4, No. 4, April 1967, pp. 511–518.

[6] "Performance of and Design Criteria for Deployable Aerodynamic Decelerators," ASD-TR-61-579, Dec. 1963, NASA.

[7] Moore, F. G., "Calculation of Nonuniform Flow Fields Over Wedges and Cones by the Method of Characteristics," MS-thesis, 1968, Virginia Polytechnic Inst., Blacksburg, Va.

[8] Nerem, R. M., "Pressure and Heat Transfer on High-Speed Aerodynamic Decelerators of the Ballute Type," *AIAA Aerodynamic Deceleration Systems Conference*, AIAA, New York, 1966.

[9] Sullivan, R. P., Donaldson, C. duP., and Hayes, W. D., "Linearized Pressure Distribution with Strong Supersonic Entropy Layers," *Journal of Fluid Mechanics*, Vol. 16, 1963, pp. 481–496.

[10] George, A. R., "Perturbations of a Plane and Axisymmetric Entropy Layers," *AIAA Journal*, Vol. 5, No. 12, Dec. 1967, pp. 2155–2159.

[11] Brooks, E. N., "Application of the Method of Integral Relations to Supersonic Nonuniform Flow Past Wedges and Cones," M. S. thesis, 1967, Virginia Polytechnic Inst., Blacksburg, Va.

[12] South, J. C., Jr., "Calculation of Axisymmetric Supersonic Flow Past Blunt Bodies with Sonic Curves, Including a Program Description and Listing," TN D-4563, 1968, NASA.

[13] Barteneu, D. A. and Shishou, V. P., "Calculation of a Nonuniform Supersonic Axisymmetric Gas Flow Past a Pointed Body of Revolution," *Aviatsionnaia Tekhnika*, No. 1, 1968, pp. 3–9.

[14] Inouye, M., "Numerical Solutions for Blunt Axisymmetric Bodies in a Supersonic Spherical Source Flow," TN D-3383, 1966, NASA.

[15] Patterson, J. L. and Lewis, A. B., "An Investigation of Nonuniform Hypersonic Free-Stream Flows About Blunt Axisymmetric Bodies," AFFDL-TR-69-57, Nov. 1969, Air Force Flight Dynamics Lab., Wright-Patterson Air Force Base, Ohio.

[16] Shapiro, A. H., *The Dynamics and Thermodynamics of Compressible Fluid Flow*, Vols. I and II, Ronald Press, New York, 1953, pp. 516–522 and 676–688.

[17] Truitt, R. W., *Hypersonic Aerodynamics*, Ronald Press, New York, 1959, Chap. 1.

[18] Sims, J. L., "Tables for Supersonic Flow Around Right Circular Cones at Zero Angle of Attack," SP-3004, 1964, NASA.

[19] Love, E. S., "Generalized-Newtonian Theory," *Journal of the Aerospace Sciences*, Vol. 26, No. 5, 1959, pp. 314–315.

[20] Blottner, F. G., "Finite-Difference Methods of Solution of the Boundary-Layer Equations," *AIAA Journal*, Vol. 8, No. 2, Feb. 1970, pp. 193–205.

[21] Rakich, J. V., "Three-Dimensional Flow Calculation by the Method of Characteristics," *AIAA Journal*, Vol. 5, No. 10, Oct. 1967, pp. 1906–1908.

DECEMBER 1971 J. SPACECRAFT VOL. 8, NO. 12

Shock-Capturing, Finite-Difference Approach to Supersonic Flows

PAUL KUTLER* AND HARVARD LOMAX†
NASA Ames Research Center, Moffett Field, Calif.

Three-dimensional, inviscid, supersonic flow containing primary and embedded shock and expansion waves is determined over and behind simple wings and wing-body combinations. The nonlinear gas-dynamic equations are differenced according to a method proposed by MacCormack which is a variation of the Lax-Wendroff technique. Progressive development toward aircraftlike configurations is made by obtaining results for the flow over cones at large incidences, conical wing-body combinations, the flow over and behind pointed ogives, cone-cylinders, and planar delta wings at angle of attack. Comparisons are made with other applicable theories and when possible with experiment.

Introduction

MANY numerical techniques used to compute supersonic flowfields about simplified configurations have been developed in recent years. These techniques are based on both the Eulerian and Lagrangian systems and their combination. No attempt is made here to mention them all or to weigh their individual merits; rather, a few of them are referenced in order to bring out a perspective for the one particular approach that was used to compute all of the cases shown in the main body of this paper. The objective is to show that this one simple, rapid, and easily applied method can be used as a "production tool" to generate accurate solutions for the flow over and behind a wide variety of wings, bodies, and wing-body combinations with surrounding and embedded shock-waves.

Two distinct approaches are used in practice to compute multishocked flows. One is referred to as a sharp-shock technique and the other as a shock-capturing technique. Sharp-shock techniques isolate all shock waves by some logical procedure and apply the Rankine-Hugoniot shock relations

Presented as Paper 71-99 at the AIAA 9th Aerospace Sciences Meeting, New York, January 25–27, 1971; submitted February 8, 1971; revision received July 19, 1971.

* Research Scientist. Member AIAA.

† Chief, Computational Fluid Dynamics Branch. Member AIAA.